



Research paper

Analysis of damage identification of self-anchor suspension bridge

Xilong Zheng¹, Di Guan², Yiqiang Wang³

Abstract: For the self-anchored suspension bridge with large span and complex structure, based on the finite element analysis and combined with the bridge load test, the stress characteristics before and after damage are analyzed in detail. For the main girder of the main vulnerable component, a variety of identification methods based on the existing dynamic damage identification methods are selected for damage identification comparison and analysis. According to the identification results of each method, an effective method for damage monitoring of the main girder of the bridge is determined. For the main girder of the vulnerable member of the self-anchored suspension bridge, according to the stress characteristics of each section and the position relationship with the assumed dynamic sensor, five damaged girder sections are set up, and each damage is assigned three levels of 10%, 20% and 40%. Based on the results of single damage and combined damage of these five girder sections, the indexes suitable for main girder damage identification are found out from various existing damage identification indexes. The Cross Modal Strain Energy (CMSE) index is selected as the main damage monitoring method for self-anchored suspension bridges because of its full damage identification ability and good noise resistance.

Keywords: self-anchored suspension bridge, damage identification, curvature mode method, flexibility matrix method

¹PhD., Harbin University, School of Intelligent and Architectural Engineering, No.109 Zhongxing Da Dao, Harbin, China, e-mail: sampson88@126.com, ORCID: [0000-0001-5571-667X](https://orcid.org/0000-0001-5571-667X)

²Msc., Harbin University, School of Intelligent and Architectural Engineering, No.109 Zhongxing Da Dao, Harbin, China, e-mail: 996349518@qq.com, ORCID: [0009-0006-2965-806X](https://orcid.org/0009-0006-2965-806X)

³Msc., Liaoning Jiaotou Maintenance Engineering Co., Ltd, General Affairs Department, No. 81 Wencui Road, China, e-mail: 1377089564@qq.com, ORCID: [0009-0005-7483-4088](https://orcid.org/0009-0005-7483-4088)

1. Introduction

Since the middle of the last century, bridge engineering technology has developed by leaps and bounds, and a large number of bridges with complex structures have emerged. Among them, self-anchored suspension bridges have become a highly competitive bridge type in the city with the advantages of novel structure, beautiful appearance, reasonable span layout and no anchorage, and have been developed and applied more at home and abroad [1, 2]. This kind of bridge structure generally includes main cable, sling, stiffening girder, main tower and other main components. The main cable is one of the main tensile elements in the structure, which mainly bears tension and shows nonlinear characteristics, and can affect the balance of the system by changing its elastic deformation and geometry [3]. Sling is a force-transmitting component that bears axial tension and transfers the self-weight and external load of stiffening girder to the main cable. However, cable towers and stiffening girders are mainly subjected to axial compression under constant load, and when live load is added, they become subjected to the combined action of compression and bending [4–7].

For the ever-increasing number of long-span bridges similar to self-anchored suspension bridges, after they are put into operation for a period of time, due to the comprehensive effects of design, construction and environment, the microstructure of materials will evolve over time, resulting in changes in structural strength, stiffness and other parameters [8–11]. As a result, cracks, corrosion, deformation and other damages have accumulated in the structure, and these minor damages often cause difficult accidents, which have a great impact on the national economy, social stability and people's lives and property [12–14].

While effectively using bridges to relieve traffic pressure, in order to ensure their safety and durability, many large bridges at home and abroad have begun to set up long-term health detection and monitoring systems, and self-anchored suspension bridges are no exception [15, 16]. In this system, the technical core and key point is how to find a damage identification method suitable for the structural damage characteristics of self-anchored suspension bridge on the basis of understanding the influence of bridge structure damage on the original structure, so as to detect the existence and location of damage in time and quickly, and further estimate the damage amount to help people repair the structure in time. This research is a hot issue at home and abroad, which has important theoretical significance and practical value.

2. Project overview

A bridge is a self-anchor suspension bridge with a steel-concrete composite beam. The span layout is 108 m + 248 m + 108 m, the main span ratio is 1 / 2.3, and the vertical span ratio of the main span is 1 / 5. The bridge elevation view is shown in Fig. 1. The design load is highway-I, the nett width of bridge deck: 2.0 m (sidewalk) + 15.5 m (roadway) + 2.0 m (middlebelt) + 15.5 m (roadway) + 2.0 m (sidewalk). The calculated driving speed is 80 km/h.

(1) Bridge tower

The bridge tower is a reinforced concrete H-type structure, the concrete grade is C50, the main height of the bridge tower is 80.5 m, and the tower column section is box type. The tower

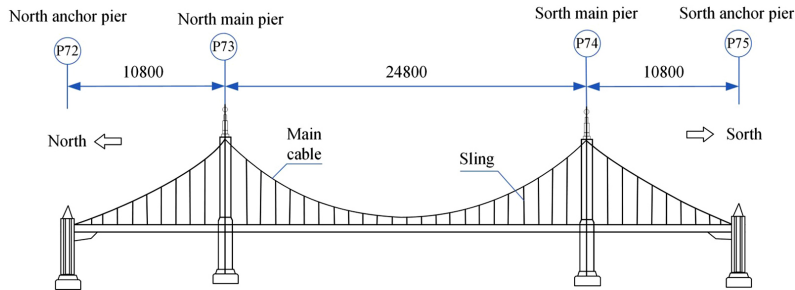


Fig. 1. Elevation view of bridge (unit: cm)

column is divided into three sections. The section size of the upper tower column is 5.4 m (length) \times 3.1 m (width), the short wall thickness is 70 cm and the long wall thickness is 55 cm. The section size of the middle tower column is 6.0 m (length) \times 3.4 m (width), short wall thickness 110 cm and long wall thickness 95 cm. The section size of the lower tower column is 8.0 m (length) and 4.4 m (width). A lower beam is set under the reinforced beam, which is a prestressed concrete structure.

(2) Stiffened beam

Stiffening girders of main span and side span are steel-concrete composite beams, and the steel deck system composed of steel main tie beams, cross beams and small longitudinal beams and the concrete deck form an integral composite section, the cross section of which is shown in Fig. 2. The deck system of steel bridge is made of Q370qE steel, which mainly depends on the stress of two main girder. The main girder is 3.2 m high (clear height inside the outer web) and 2.1 m wide (clear width inside the web), and connected by I-beams. The full width of the bridge floor is 40 m, and the standard thickness is 25 cm.

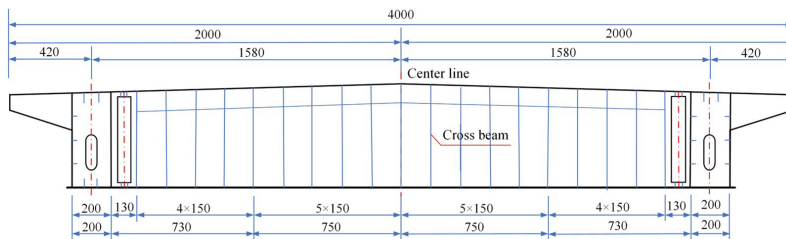


Fig. 2. Cross-sectional view of stiffening girder (unit: cm)

(3) Main cable and derrick

There are two main cables in the whole bridge, which are arranged in space. The standard strength of main cable steel wire is 1670 MPa, and the designed elastic modulus is 2.0×10^5 MPa. The vertical span ratio of the main span of the completed bridge is 1/5. According to the mechanical characteristics, they are divided into two specifications: $\varphi 7 \times 55$ and $\varphi 7 \times 91$. The numbers of suspenders increase from the bridge tower to each span: the southern half span is FS1–FS10, and the northern half span is FN1–FN10.

3. Establishment of finite element analysis model

Establishing finite element model by Midas/Civil. The bottom consolidation boundary condition is adopted for the bridge tower. The boundary constraint of main girder is realized by general support. Rigid master-slave constraints are used to connect the anchor point of the main cable, the main cable at the main cable saddle and the connection between the suspender and the stiffening girder. The whole bridge is divided into 2164 units and 1980 nodes. There are 104 main cable units and 98 suspender units, all of which are non-bending members, using cable units and truss units respectively. The finite element model is shown in Fig. 3.



Fig. 3. Finite element model of self-anchored suspension bridge

4. Damage condition

It has been many years of theoretical experimental research on damage identification by dynamic method, and the technology has become increasingly mature, and the effectiveness of each identification method has also been widely and deeply studied. Here, the curvature mode method and flexibility matrix method with good identification effect are selected to identify the damage of the main girder of self-anchored suspension bridge. In order to make the simulation analysis results more practical and reasonable, it is assumed that 53 sensors are arranged on each side of the main tie beam at a longitudinal interval of about 8m, which are located on the corresponding unit nodes, and the sensor numbers are 1–53 from south to north, as shown in Fig. 4.

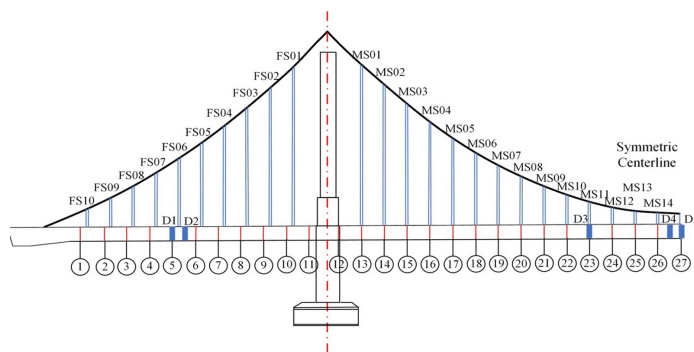


Fig. 4. Schematic diagram of dynamic measuring point arrangement and damage location of the whole bridge

In the above Figures, the beam segments of D1–D5 at the set damage position are indicated at the same time, and the damage is caused by the load-bearing main tie beams on the upstream and downstream sides simultaneously. Wherein D1, D3 and D5 coincide with the dynamic measuring points, and are respectively selected in the middle of the side span, 3/8 point of the main span and the middle of the main span according to the maximum stress position and damage proximity of the structure. D2 and D4 are located between the measuring points of two dynamic sensors, so as to study the dynamic damage identification effect when the damage is close to the measuring point and far away from the measuring point. At the damaged beam section, the damage of the structure is simulated by reducing the elastic modulus of the element within 2 m, and the damage degree is divided into three levels according to 10%, 20% and 40%.

5. Single damage identification

When the damage of each beam segment occurs independently, the existence of the damage can be judged according to the frequency change used for global damage identification and the Moving Average Convergence (MAC) quasi-side. Taking the second mode as an example, the global identification results are shown in Table 1.

Table 1. Frequency and MAC value under each single damage

Damaged beam segment	Frequency value (Hz)			MAC value		
	10% damage	20% damage	40% damage	10% damage	20% damage	40% damage
D1	0.390336	0.390192	0.389763	0.999967	0.999837	0.998940
D2	0.390386	0.390304	0.390057	0.999986	0.999928	0.999507
D3	0.390415	0.390365	0.390197	0.999893	0.999431	0.995229
D4	0.390414	0.390366	0.390224	0.999998	0.999991	0.999936
D5	0.390376	0.390281	0.390002	0.999999	0.999997	0.999975

As can be seen from the above table, the distribution of bridge frequency and MAC value in lossless condition is 0.390452 Hz and 1. Both the bridge frequency and MAC value in the table decrease, indicating the existence of damage to the stiffened beam. The reduction of the value can still reflect the degree of damage on the whole, but the localization and local quantification of damage need further identification of the selected damage indexes.

5.1. Curvature modal method

With a limited number of sensors actually monitored, the calculation of curvature mode can not be directly obtained by the second derivative of structural mode shape function, and the central difference calculation should be carried out by using the mode shapes at the measuring points of each sensor. However, after the damage is enough, the vibration mode used in the calculation should change greatly near the damage, while other measuring points change little, which requires the standardized treatment of the damaged vibration mode.

For the curvature modal values of each order, due to the different distribution of vibration mode vectors after each order specification, it is bound to lead to different distribution trends and form multiple damage identification indexes. In practical application, considering that the low-order vertical component vibration mode is easy to measure, the second-order vertical bending and fourth-order torsional vibration mode of the self-anchored suspension bridge with a large proportion of vertical vibration mode components are selected to calculate the curvature mode value under the damage of each beam section. The second-order mode is shown in Figs. 5–9.

From Fig. 5 to Fig. 9, it can be seen that when the beam segments D1, D3 and D5 located at the measuring point are damaged in three different degrees, the curvature modal value curve under the selected mode will have a single point sharp mutation at the damage measuring point; However, when the non-measuring-point beam segments D2 and D4 are damaged to the same extent, the measuring points at both ends will form abrupt regions on the curvature modal value curve, and both abrupt values will increase with the aggravation of the damage degree, indicating that the selected two-order structural curvature modal is sensitive to the damage of the main beam. In order to make the abrupt change of curvature mode more obvious under small-scale damage, we can use the Cross Modal Strain Energy (CMSE) index of loss curvature mode difference introduced in Chapter 2 for further damage identification, in which the damage location is carried out by using the index (Z_f) value in Fig. 10–14.

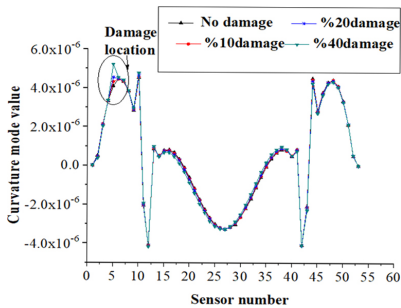


Fig. 5. Curvature modal value of beam segment D1 damage

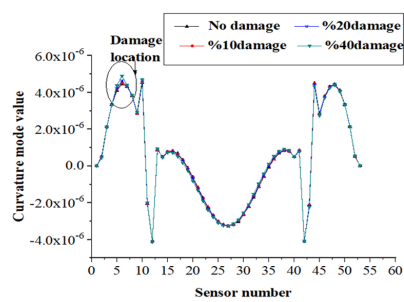


Fig. 6. Curvature modal value of damage beam segment D2 damage

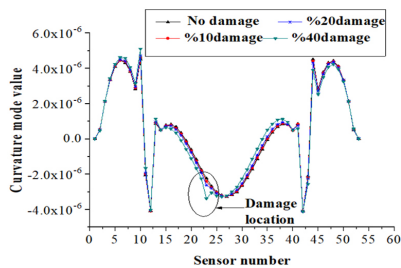


Fig. 7. Curvature modal value of beam segment D3 damage

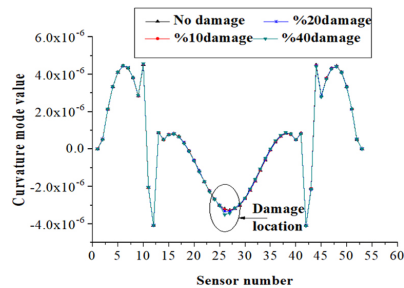


Fig. 8. Curvature modal value of beam segment D4 damage

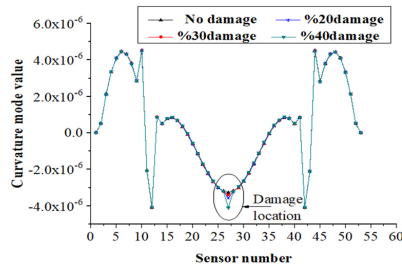


Fig. 9. Curvature modal value of beam segment D5 under damage

From Fig. 10 to Fig. 14, it can be seen that for the beam damage at the measuring point, the Z_f values of the two modes can well identify the damage locations under different damage levels under the condition of multi-peaks; However, when the same damage occurs between two sensors, the 10% loss at D2 can only be correctly identified by the judgment value in the fourth-order curvature mode, which shows that the fourth-order CMSE index has a better identification effect, and as shown in Fig. 15, it has a peak value far greater than that at other points, and there is no interference peak, so it can accurately appear a mutation domain and directly determine a smaller identifiable damage domain.

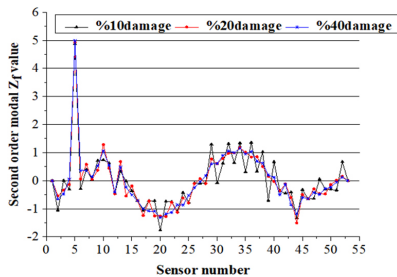


Fig. 10. Z_f value of the second mode under the damage of beam section D1

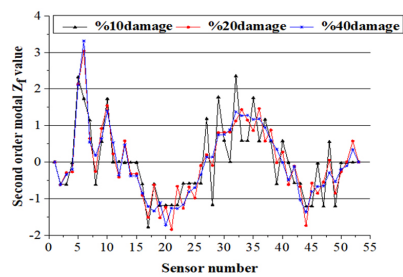


Fig. 11. Z_f value of the second mode under the damage of beam section D2

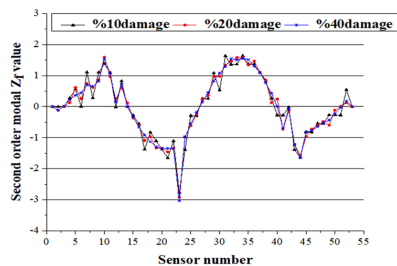


Fig. 12. Z_f value of the second mode under the damage of beam segment D3

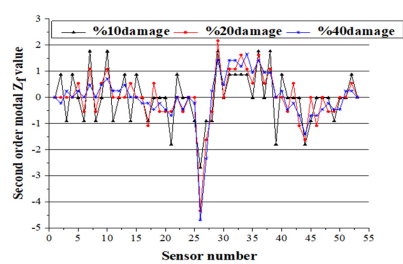


Fig. 13. Z_f value of the second mode under the damage of beam segment D4

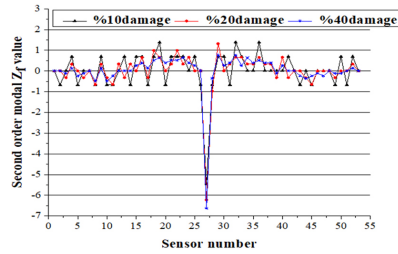


Fig. 14. Z_f value of second mode under damage of beam segment D5

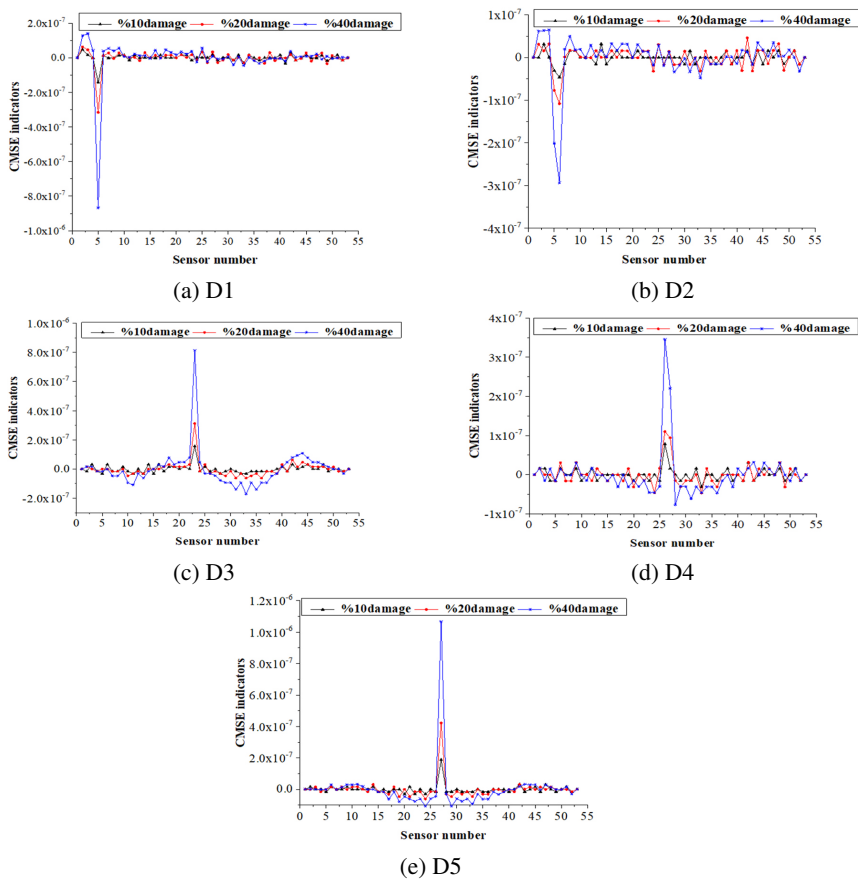


Fig. 15. CMSE index of fourth-order mode under damage of beam segments D1–D5: (a) D1, (b) D2, (c) D3, (d) D4, (e) D5

In addition, for the three kinds of damage degrees at the same damage place in the above Figures, the CMSE index values at the damage peak point are shown in Table 2. Although the distribution is non-linear, the sizes can be clearly distinguished. When the median damage

degree in the table is subdivided, the damage degree comparison database of CMSE index can be established accordingly, so as to realize damage quantification.

Table 2. Peak point of CMSE index under damage

Harm degree	Damaged beam section $\times 10^{-7}$				
	D1 damage Peak point	D2 damage Peak point	D3 damage Peak point	D4 damage Peak point	D5 damage Peak point
10%	-1.42	-0.46	1.56	0.78	1.88
20%	-3.16	-1.08	3.13	1.10	4.23
40%	-8.68	-2.94	8.13	3.45	10.66

5.2. Flexibility matrix method

Flexibility matrix belongs to the whole modal quantity, which can be accurately established by all the degrees of freedom and modal values of the structure in theory. However, in real bridge engineering, the flexibility matrix can only be established approximately due to the limitation of the number of sensors and measurement technology for modal measurement. Nevertheless, due to the fact that the flexibility matrix contains the reciprocal of the frequency square, the contribution of each modal quantity to it decreases rapidly with the increase of modal order, and it can be established accurately by using several low-frequency vibration modes of the structure, and the actual extraction accuracy is higher for low-order modes, which is more practical.

Therefore, the flexibility matrix of the main girder of the self-anchored suspension bridge is established from the reality by using the first four low-frequency vertical vibration mode components, and the numerical value in the intact state is shown in Fig. 16.

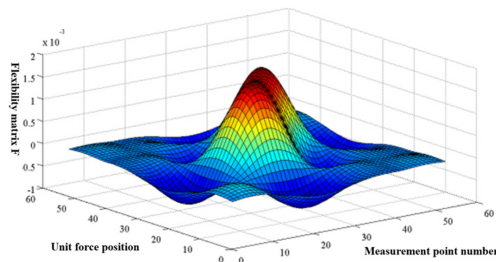


Fig. 16. Flexibility matrix of lossless structure

In the Fig., the horizontal X coordinate represents the degrees of freedom of each row of measuring points in the flexibility matrix F, while the vertical Y coordinate represents the degrees of freedom of each column of measuring points acted by unit force.

However, when the D1–D5 beam segments of the structure are damaged to 10%, the overall flexibility matrix will change before and after the damage, resulting in the difference matrix as shown in Fig. 17.

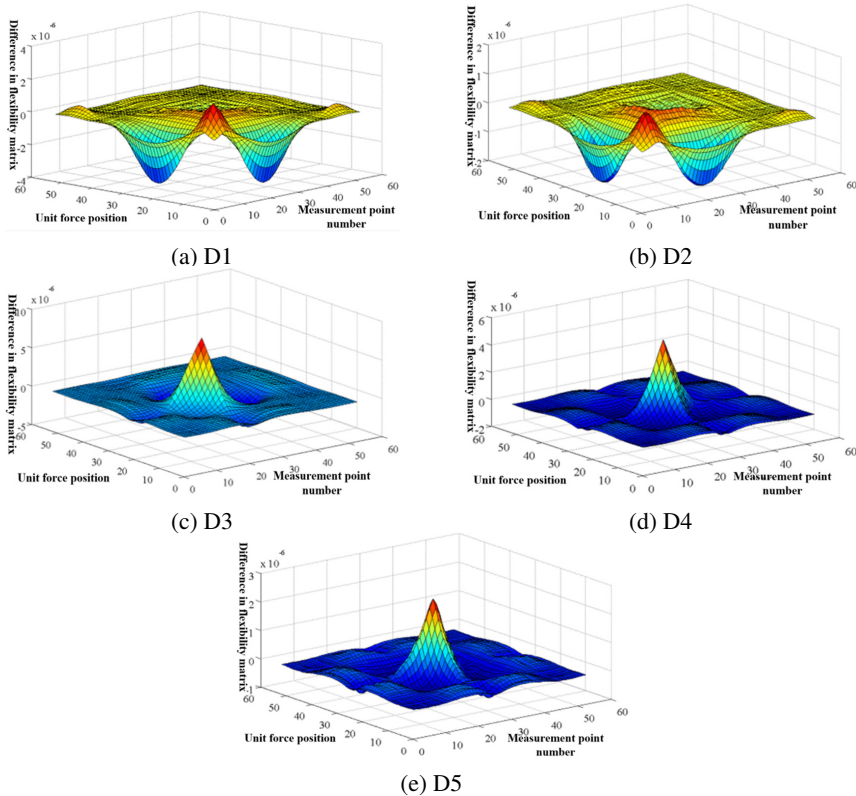


Fig. 17. Difference of flexibility matrix of beam segments D1–D5 after 10% damage:
(a) D1, (b) D2, (c) D3, (d) D4, (f) D5

As can be seen from Fig. 17, the difference of flexibility matrix will have a peak at the diagonal of the matrix after damage at different positions, and from the specific coordinates of the peak points in Table 3, it can be seen that their correspondence with their respective damage positions or damage domains conforms to the physical meaning of diagonal elements, that is, the response value of the degree of freedom at the measuring point to the unit force directly acting on it is relatively large.

For the damage set in this section, the calculated Flexibility Matrix Difference (MFD) index of the corresponding degrees of freedom of each measuring point of the main beam is shown in Fig. 18. In the Fig. 18, the MFD index will form a peak with multiple non-destructive measuring points at the peak around the damage point or adjacent measuring points, which makes the damage point not prominent, resulting in the existence of measuring points near the maximum peak point for both the damage at the measuring points and the damage between the measuring points, thus only the damage domain can be identified, which is not conducive to the rapid identification of the damage at the measuring points. In addition, as can be seen in the following Fig. 18(a) and Fig. 18(b), when the side span represents moderate or above damage to the beam section, the value is close to the non-damage peak, which is easy to cause misjudgment of damage.

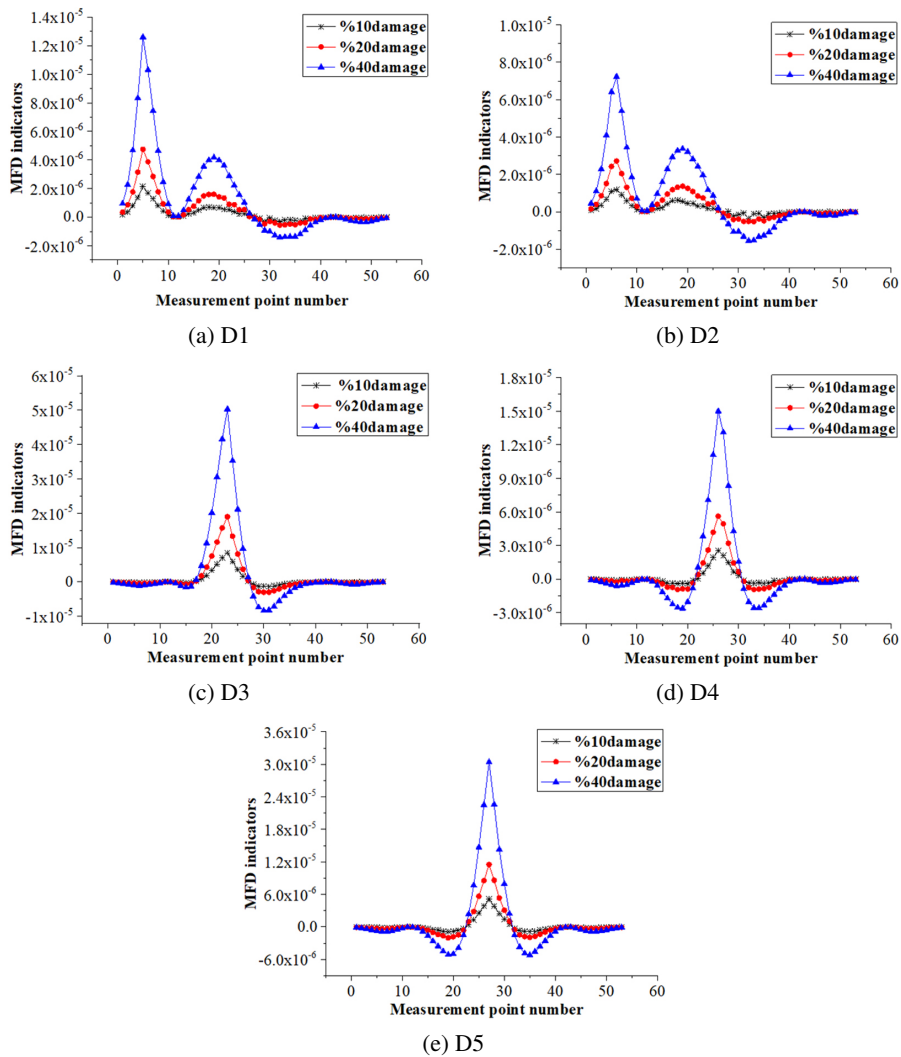


Fig. 18. MFD index of beam section D1–D5 damaged: (a) D1, (b) D2, (c) D3, (d) D4, (f) D5

Table 3. Coordinates of peak point of flexibility matrix variation

Peak value coordinate	Damaged beam segment				
	D1	D2	D3	D4	D5
X coordinate	5	6	23	26	27
Y coordinate	5	6	23	26	27

5.3. Modal strain energy method

For the calculation of modal strain energy, if the main beam unit is divided according to the actual sensor arrangement, the long length of the unit will bring a large error, so the measurement of the strain energy is the function of the curvature mode for the calculation mode $(\varphi_i''(x))^2$, but considering that the fourth curvature mode has a prominent effect on damage, the numerical curve of each measurement point index under the single damage of D1–D5 beam section, as shown in Fig. 19.

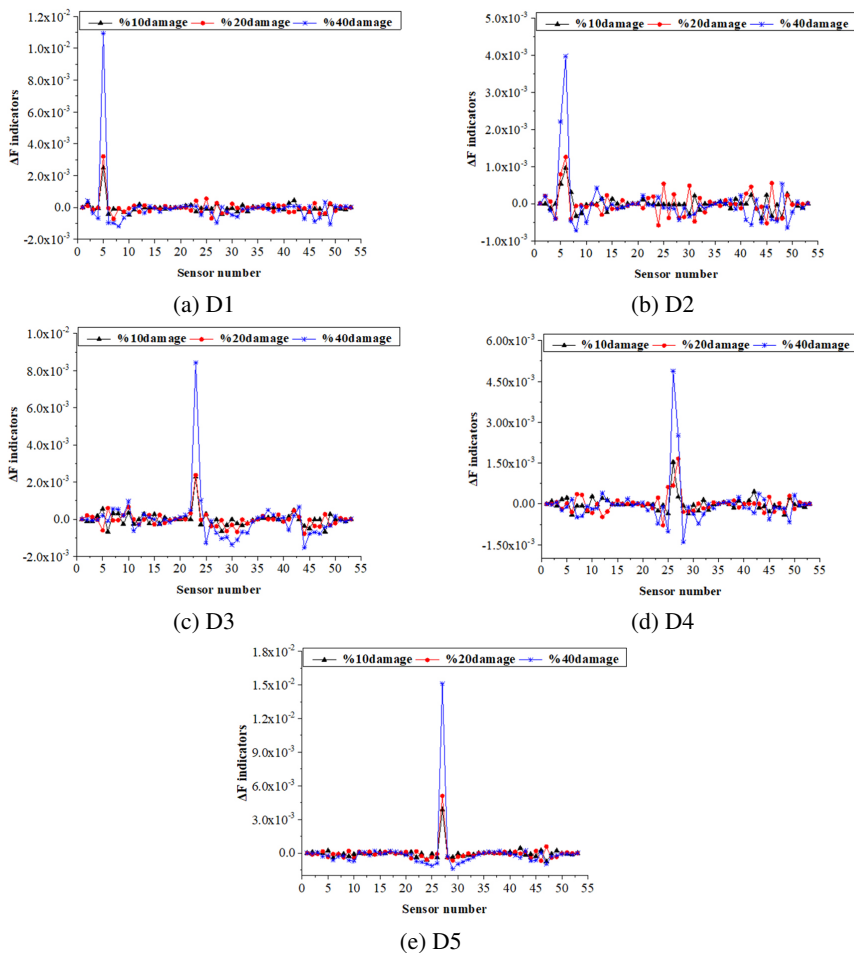


Fig. 19. Fourth-order modal index of damaged beam segments D1–D5:

(a) D1, (b) D2, (c) D3, (d) D4, (f) D5

For the calculation of modal strain energy, if it is carried out according to the main beam unit divided by the actual sensor arrangement, it's too long unit length will bring great error, so in this paper, the measuring point unit is set within 1m of the measuring point, and in

practice, only the strain energy can be measured and calculated, and the obtained strain energy is expressed as: Because the modal strain energy is a function of curvature mode, it has multi-order calculation modes, but considering that the fourth-order curvature mode has a good effect on highlighting the damage, it is selected as the calculation mode. The numerical curves of indicators at each measuring point under the single damage of D1–D5 beam segments are obtained, and the ΔF indicators are shown in Fig. 19.

Through the curve distribution of damage index values in Fig. 19, it can be found that the maximum peak values of indexes under different degrees of damage all occur at the damaged beam segment or near the measuring point, which can form a peak for damage identification. When the damage occurs at the measuring point and the damage degree of the non-measuring point is heavy, the value of the other measuring points is far less than the peak value, and the damage location can be identified. However, for D2 and D4 beams with slight damage, the index is similar to MFD index, and the damage domain cannot be completely identified. In addition, the peak value of the index corresponding to 10% and 20% damage of the same beam position is close, indicating that the index is not suitable for the quantification of small-scale damage.

6. Conclusions

1. The selected CMSE index of the fourth-order curvature mode of the main girder, which is easy to obtain in practice, has different identification effects on the damage of the main girder of the bridge. Among them, the second-order modal index will be affected by the interference peak in most damage cases, and it is necessary to identify the damage with the help of Z_f judgment value with approximate numerical distribution law, and even if the index judgment value is used, there are still some phenomena that individual or combined damage between some lighter measuring points cannot be identified.
2. Considering the comparative analysis results of the damage identification effects of each index and the advantages of dynamic damage identification, the curvature mode CMSE index can be used as the main damage monitoring means of self-anchored suspension bridge main girder. It not only has the most ideal theoretical identification effect among the selected damage identification indexes, but also has good noise resistance and practicability. Even if the main beam is slightly damaged by 10%, it can be accurately judged under a certain noise level.
3. After considering the noise error in the actual modal measurement, the curvature mode CMSE index can identify the damage of the beam section at the measuring point with 2–3% noise level when the damage is 10%; However, when the damage is doubled, the noise resistance of the index is obviously increased. At the same time, the identifiable noise level of the damage between the measuring points is raised to one level, which shows good noise resistance, which makes the CMSE index have a certain practical significance on the basis of its good theoretical damage location and quantitative ability.

References

- [1] Y. An, E. Chatzi, et al., “Recent progress and future trends on damage identification methods for bridge structures”, *Structural Control and Health Monitoring*, vol. 26, no. 10, 2019, doi: [10.1002/stc.2416](https://doi.org/10.1002/stc.2416).
- [2] T.Y. Qi, C. Wang, et al., “Mechanical behavior improving study of concrete deck of main beam at pylon root of composite beam cable-stayed bridge”, *Archives of Civil Engineering*, vol. 70, no. 2, pp. 271–289, 2024, doi: [10.24425/ace.2024.149863](https://doi.org/10.24425/ace.2024.149863).
- [3] W.R. Wickramasinghe, D.P. Thambiratnam, et al., “Vibration characteristics and damage detection in a suspension bridge”, *Journal of Sound and Vibration*, vol. 375, pp. 254–274, 2016, doi: [10.1016/j.jsv.2016.04.025](https://doi.org/10.1016/j.jsv.2016.04.025).
- [4] Y. An, B.F. Spencer, and J. Ou, “A test method for damage diagnosis of suspension bridge suspender cables”, *Computer-Aided Civil and Infrastructure Engineering*, vol. 30, no. 10, pp. 771–784, 2015, doi: [10.1111/mice.12144](https://doi.org/10.1111/mice.12144).
- [5] Z. Chen, S. Zhu, et al., “Damage detection in long suspension bridges using stress influence lines”, *Journal of Bridge Engineering*, vol. 20, no. 3, 2015, doi: [10.1061/\(ASCE\)BE.1943-5592.0000681](https://doi.org/10.1061/(ASCE)BE.1943-5592.0000681).
- [6] M. Fanhao, M. Bilal, et al., “Damage detection in active suspension bridges: an experimental investigation”, *Sensors*, vol. 18, no. 9, art. no. 3002, 2018, doi: [10.3390/s18093002](https://doi.org/10.3390/s18093002).
- [7] M. Domaneschi, M. P. Limongelli, and L. Martinelli, “Vibration based damage localization using MEMS on a suspension bridge model”, *Smart Structures and Systems*, vol. 12, no. 6, pp. 679–694, 2013, doi: [10.12989/ss.2013.12.6.679](https://doi.org/10.12989/ss.2013.12.6.679).
- [8] W. Smyth, J. Pei, and S.F. Masri, “System identification of the Vincent Thomas suspension bridge using earthquake records”, *Earthquake Engineering and Structural Dynamics*, vol. 32, no. 3, pp. 339–367, 2003, doi: [10.1002/eqe.226](https://doi.org/10.1002/eqe.226).
- [9] N.N. Long, N.H. Quyet, et al., “Damage Identification of Suspension Footbridge Structures using New Hunting-based Algorithms”, *Engineering, Technology and Applied Science Research*, vol. 13, no. 4, pp. 11085–11090, 2023, doi: [10.48084/etasr.5983](https://doi.org/10.48084/etasr.5983).
- [10] N. Tomonori, M. Abe, et al., “Structural identification of a nonproportionally damped system and its application to a full-scale suspension bridge”, *Journal of Structural Engineering*, vol. 131, no. 10, pp. 1536–1545, 2005, doi: [10.1061/\(ASCE\)0733-9445\(2005\)131:10\(1536\)](https://doi.org/10.1061/(ASCE)0733-9445(2005)131:10(1536)).
- [11] D.M. Siringoringo and Y. Fujino, “System identification of suspension bridge from ambient vibration response”, *Engineering Structures*, vol. 30, no. 2, pp. 462–477, 2008, doi: [10.1016/j.engstruct.2007.03.004](https://doi.org/10.1016/j.engstruct.2007.03.004).
- [12] F. Ubertini, “On damage detection by continuous dynamic monitoring in wind-excited suspension bridges”, *Meccanica*, vol. 48, pp. 1031–1051, 2013, doi: [10.1007/s11012-012-9650-2](https://doi.org/10.1007/s11012-012-9650-2).
- [13] X. Youlin, Z. Chaodong, et al., “Multi-level damage identification of a bridge structure: a combined numerical and experimental investigation”, *Engineering Structures*, vol. 156, pp. 53–67, 2018, doi: [10.1016/j.engstruct.2017.11.014](https://doi.org/10.1016/j.engstruct.2017.11.014).
- [14] C. Miao, M. Wang, et al., “Damage alarming of long-span suspension bridge based on GPS-RTK monitoring”, *Journal of Central South University*, vol. 22, no. 7, pp. 2800–2808, 2015, doi: [10.1007/s11771-015-2811-4](https://doi.org/10.1007/s11771-015-2811-4).
- [15] L. Materazzi and F. Ubertini, “Eigenproperties of suspension bridges with damage”, *Journal of Sound and Vibration*, vol. 330, no. 26, pp. 6420–6434, 2011, doi: [10.1016/j.jsv.2011.08.007](https://doi.org/10.1016/j.jsv.2011.08.007).
- [16] C. Zhiwei, C. Qinlin, and L. Jun, “Stress influence line identification of long suspension bridges installed with structural health monitoring systems”, *International Journal of Structural Stability and Dynamics*, vol. 16, no. 04, art. no. 1640023, 2016, doi: [10.1142/S021945541640023X](https://doi.org/10.1142/S021945541640023X).

Received: 2024-05-29, Revised: 2024-07-17